

Modeling the Interconnection of a Pseudo-Differential Link Using a Wide Return Conductor

Frédéric Broydé and Evelyne Clavelier
 Excem
 Maule, France
 fredbroyde@eurexcem.com

Abstract

A type of pseudo-differential link uses a floating termination circuit connected to an interconnection comprising a return conductor wider than the transmission conductors. For n channels, the link is designed using a per-unit-length (p.u.l.) impedance matrix and a p.u.l. admittance matrix, both of size $n \times n$. The paper establishes the relationship between this model and an alternative model which uses a p.u.l. impedance matrix and a p.u.l. admittance matrix of size $(n+1) \times (n+1)$. In the process, we define two vectors which may be used to assess external crosstalk.

I. Introduction

A type of pseudo-differential link (PDL) providing $n \geq 2$ channels uses a multiconductor interconnection having n transmission conductors (TCs) and a wide return conductor distinct from the reference conductor (ground) [1] [2]. In the intended mode of operation of the PDL, the electric and magnetic fields of the signals are mainly confined between the TCs and the return conductor, so that the return current caused by signal propagation flows mainly in the return conductor. This is for instance obtained if one of the two interconnection-ground structures shown in Fig. 1 is used with a floating termination circuit connected to the TCs and to the return conductor. This configuration, known as the ZXnoise method, is intended to provide a reduced echo and an enhanced protection against external crosstalk (external crosstalk is the crosstalk between one or more channels of the PDL and other circuits).

If the return conductor behaves as an ideal electromagnetic screen, only the TCs and the return conductor need to be taken into account to model propagation in the interconnection. This lead to a $(n+1)$ -conductor multiconductor transmission line (MTL) model. The design procedure defined for the ZXnoise method [1] [2] is based on this model, which involves matrices of size $n \times n$. Taking into account the reference conductor, we may also use a $(n+2)$ -conductor MTL model. The relationships between the two MTL models have only been established in the special case of ideal electric and magnetic shielding by the return conductor [1].

This paper is about the matrices which define the $(n+1)$ -conductor and $(n+2)$ -conductor MTL models of an interconnection used according to the ZXnoise method, when the assumption of ideal shielding is removed. This investigation will lead us to define two vectors which characterize the shielding performance of the return conductor and may consequently be used to assess the residual external crosstalk in the framework of the $(n+1)$ -conductor MTL model.

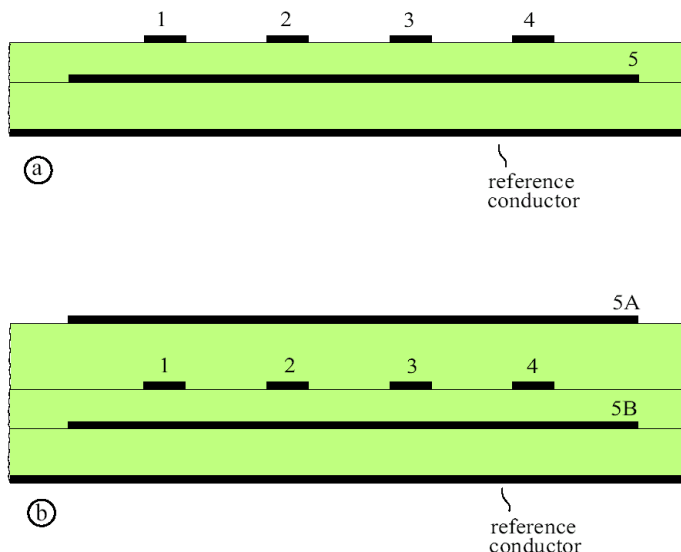


Fig. 1. Two possible cross-sections for an interconnection-ground structure intended to be used in a PDL implementing the ZXnoise method, where 1 to 4 are the TCs, where 5 is the return conductor in a and where the return conductor in b is made of 5A and 5B.

II. Matrices defining the $(n+1)$ -conductor MTL model

Let us investigate the electrical characteristics of an interconnection intended to operate according to the ZXnoise method. We consider an electrically short segment of the interconnection, of length Δz , for which we want to define the per-unit-length (p.u.l.) impedance matrix with respect to the return conductor, denoted by \mathbf{Z}_R , and the p.u.l. admittance matrix with respect to the return conductor, denoted by \mathbf{Y}_R . These matrices are symmetrical $n \times n$ matrices defined by theoretical measurement configurations shown in Fig. 2 and 3. Note that, in Fig. 2 and 3, the return conductor is shown as a cylindrical shell containing the TCs, but this geometry is not assumed in any way.

\mathbf{Z}_R may be measured with the theoretical setup shown in Fig. 2a, in which a current i is injected by a current source connected between the TC number α and the return conductor. At the near-end (on the left), the natural voltages referenced to the return conductor, denoted by $v_{R1\alpha}$ to $v_{Rn\alpha}$, are measured to obtain the entries $Z_{R1\alpha}$ to $Z_{Rn\alpha}$ of \mathbf{Z}_R , respectively, using

$$Z_{R\beta\alpha} = \frac{v_{R\beta\alpha}}{i \Delta z} \quad (1)$$

At the far-end of the segment of interconnection being measured (on the right), the TCs are connected to the return conductor. At

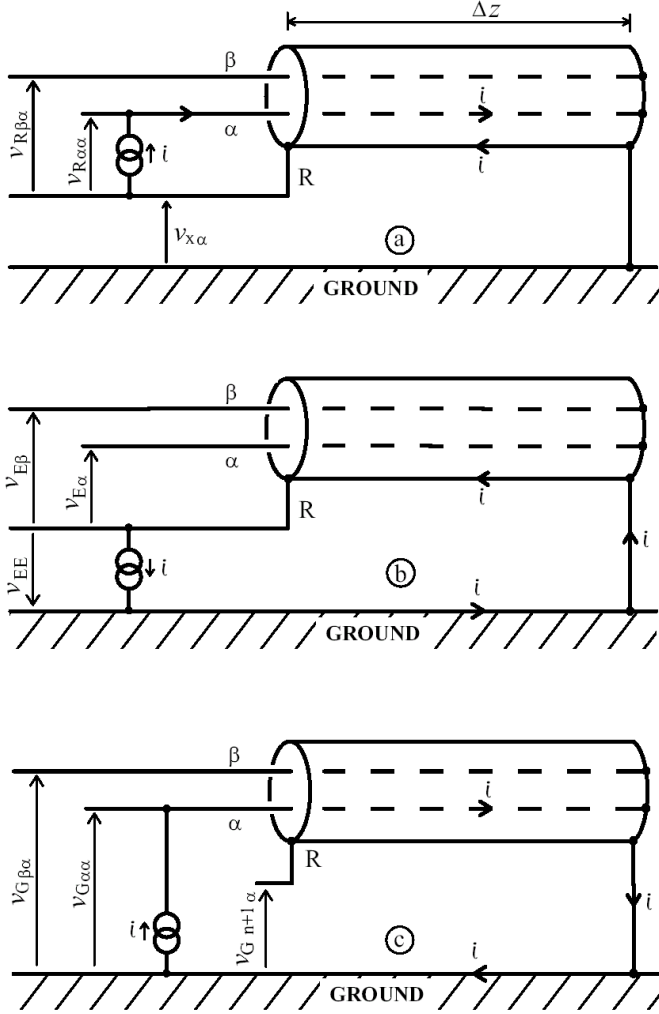


Fig. 2. Measurement of the p.u.l. impedance parameters. R denotes the return conductor. Only the TCs number α and β are shown.

the far-end, the connection between the return conductor and the reference conductor is not strictly necessary for the measurement of Z_R , but the presence of this connection allows the definition of the voltage $v_{X\alpha}$ between the return conductor and the reference conductor, at the near-end.

Y_R may conceptually be measured with the theoretical setup shown in Fig. 3a, in which a voltage v is applied by a voltage source connected between the TC number α and the return conductor. At the near-end, the natural currents $i_{R1\alpha}$ to $i_{Rn\alpha}$ are measured to obtain the entries $Y_{R1\alpha}$ to $Y_{Rn\alpha}$ of Y_R , respectively, using

$$Y_{R\beta\alpha} = \frac{i_{R\beta\alpha}}{v \Delta z} \quad (2)$$

At the far-end, the TCs and the return conductor are floating. At the near-end, the current $i_{X1\alpha}$ flowing out of the return conductor is not necessary for the measurement of Y_R , but it is important to note that this current is not necessarily equal to $i_{R1\alpha} + \dots + i_{Rn\alpha}$. Consequently, we introduce the current $i_{X2\alpha}$ flowing out of the interconnection, this current being given by

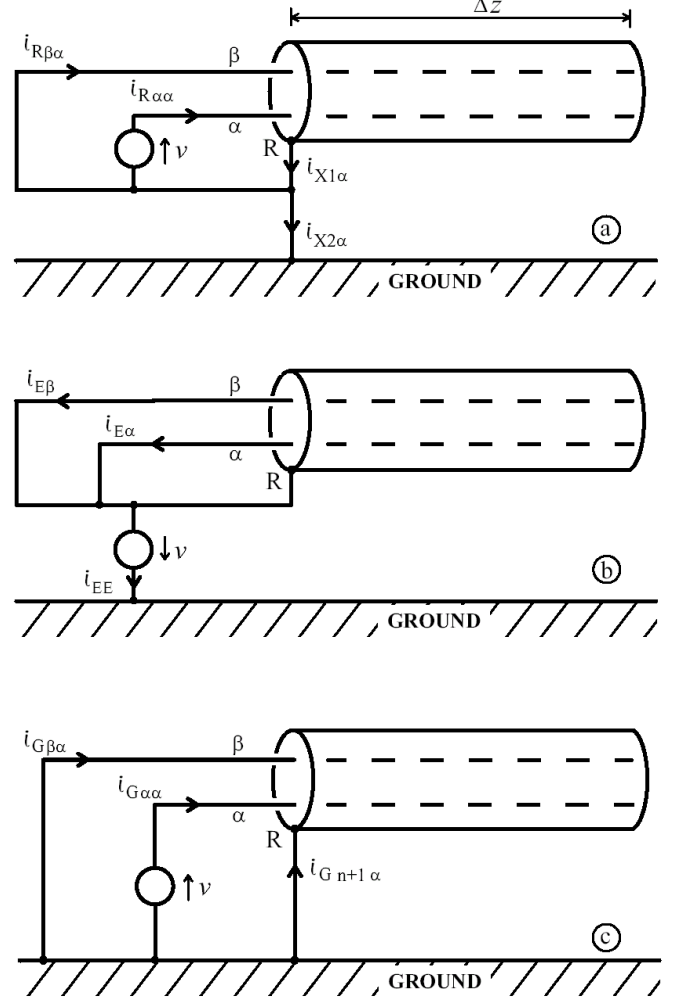


Fig. 3. Measurement of the p.u.l. admittance parameters. R denotes the return conductor. Only the TCs number α and β are shown.

$$i_{X2\alpha} = i_{X1\alpha} - v \Delta z \sum_{\beta=1}^n Y_{R\beta\alpha} \quad (3)$$

III. Shielding action of the return conductor

Any conductor may provide a shielding action. The setup shown in Fig. 2b is adequate for the assessment of the shielding action of the return conductor when a current source injects a current $-i$ into the return conductor. In this case, a good shielding effectiveness corresponds to low induced voltages referenced to the return conductor v_{E1} to v_{En} measured at the near-end. We may define the p.u.l. coupling impedances Z_{E1} to Z_{En} and the p.u.l. external impedance Z_{EE} as

$$Z_{EE} = \frac{v_{EE}}{i \Delta z} \quad \text{and} \quad \forall \alpha \quad Z_{E\alpha} = \frac{v_{E\alpha}}{i \Delta z} \quad (4)$$

Because of reciprocity, the circuit of Fig. 2a is such that

$$\forall \alpha \quad v_{X\alpha} = -Z_{E\alpha} i \Delta z \quad (5)$$

The setup shown in Fig. 3b is adequate for the assessment of the shielding action of the return conductor when a voltage source applies a voltage $-v$ to the return conductor. In this case, a good shielding effectiveness corresponds to low induced currents i_{E1} to i_{En} measured at the near-end. We may define the p.u.l. coupling admittances Y_{E1} to Y_{En} and the p.u.l. external admittance Y_{EE} as

$$Y_{EE} = \frac{i_{EE}}{v \Delta z} \quad \text{and} \quad \forall \alpha \quad Y_{E\alpha} = \frac{i_{E\alpha}}{v \Delta z} \quad (6)$$

Because of reciprocity, the circuit of Fig. 3a is such that

$$\forall \alpha \quad i_{X2\alpha} = -Y_{E\alpha} v \Delta z \quad (7)$$

If the return conductor was a circular cylindrical shell and the ground conductor was a coaxial circular cylinder, the $Z_{E\alpha}$ would be the p.u.l. transfer impedances of the interconnection and the $Y_{E\alpha}$ would be the p.u.l. transfer admittances of the interconnection in this particular configuration [3] [4]. This would still be the case in any non-circular-symmetrical configuration where only type 1 and type 2 couplings are present [5].

IV. Matrices defining the $(n+2)$ -conductor MTL model

The p.u.l. impedance matrix with respect to ground, denoted by \mathbf{Z}_G , is a symmetrical $(n+1) \times (n+1)$ matrix. It may conceptually be measured with the theoretical setup shown in Fig. 2c, in which a current i is injected by a current source connected between the TC number α and ground, or between the return conductor and ground. At the near-end (on the left), the natural voltages referenced to ground $v_{G1\alpha}$ to $v_{Gn+1\alpha}$ are measured to obtain the entries $Z_{G1\alpha}$ to $Z_{Gn+1\alpha}$ of \mathbf{Z}_R , respectively, using

$$Z_{G\beta\alpha} = \frac{v_{G\beta\alpha}}{i \Delta z} \quad (8)$$

At the far-end, the TCs and the return conductor are grounded. For the case where the current source is connected to the return conductor, a comparison of Fig. 2b and Fig. 2c shows that

$$Z_{Gn+1n+1} = Z_{EE} \quad (9)$$

and, for $1 \leq \alpha \leq n$,

$$Z_{Gn+1\alpha} = Z_{G\alpha n+1} = Z_{EE} - Z_{E\alpha} \quad (10)$$

For the case where the current source is connected to one of the TCs, we see that the setup shown in Fig. 2c is a superposition of the setups shown in Fig. 2a and Fig. 2b after a sign reversal. Consequently, for $1 \leq \alpha \leq n$ and $1 \leq \beta \leq n$,

$$Z_{G\alpha\beta} = Z_{R\alpha\beta} + Z_{EE} - Z_{E\alpha} - Z_{E\beta} \quad (11)$$

where (5) was used.

The p.u.l. admittance matrix with respect to ground, denoted by \mathbf{Y}_G , is a symmetrical $(n+1) \times (n+1)$ matrix. It may conceptually be measured with the theoretical setup shown in Fig. 3c, in which a voltage v is applied by a voltage source connected between the TC number α and ground. At the near-end, the natural currents $i_{G1\alpha}$ to $i_{Gn\alpha}$ are measured to obtain the entries $Y_{G1\alpha}$ to $Y_{Gn\alpha}$ of \mathbf{Y}_G , respectively, using

$$Y_{G\beta\alpha} = \frac{i_{G\beta\alpha}}{v \Delta z} \quad (12)$$

At the far-end of the segment of interconnection being measured, the TCs and the return conductor are floating. For the case where the voltage source is connected to one of the TCs, a comparison of Fig. 3a and Fig. 3c shows that, for $1 \leq \alpha \leq n$ and $1 \leq \beta \leq n$,

$$Y_{G\alpha\beta} = Y_{R\alpha\beta} \quad (13)$$

and

$$Y_{Gn+1\alpha} = Y_{G\alpha n+1} = -\frac{i_{X1\alpha}}{v \Delta z} \quad (14)$$

using (3) and (7), we obtain

$$Y_{Gn+1\alpha} = Y_{G\alpha n+1} = Y_{E\alpha} - \sum_{\beta=1}^n Y_{R\beta\alpha} \quad (15)$$

For the case where the voltage source is connected to the return conductor, we see that the setup shown in Fig. 3c is a superposition of the setup shown in Fig. 3b after a sign reversal and, for each value $\alpha = 1$ to $\alpha = n$, of one setup shown in Fig. 3a after a sign reversal. Consequently

$$Y_{Gn+1n+1} = Y_{EE} - \sum_{\alpha=1}^n Y_{E\alpha} + \sum_{\alpha=1}^n \frac{i_{X1\alpha}}{v \Delta z} \quad (16)$$

using (3) and (7), we obtain

$$Y_{Gn+1n+1} = Y_{EE} + \sum_{\alpha=1}^n \sum_{\beta=1}^n Y_{R\beta\alpha} - 2 \sum_{\alpha=1}^n Y_{E\alpha} \quad (17)$$

At this stage, we have obtained:

- all entries of the matrix \mathbf{Z}_G as a function of the matrix \mathbf{Z}_R , of the vector \mathbf{Z}_E and of the scalar Z_{EE} ;
- all entries of the matrix \mathbf{Y}_G as a function of the matrix \mathbf{Y}_R , of the vector \mathbf{Y}_E and of the scalar Y_{EE} .

The interconnection may be accurately modeled as a $(n+1)$ -conductor MTL having no interaction with the external world if and only if we may, in a given configuration, to a sufficient accuracy, consider that $\mathbf{Z}_E \approx \mathbf{0} \Omega$ and $\mathbf{Y}_E \approx \mathbf{0} \text{ S}$. In this case, using (9), (10), (11), (13), (15) and (17), we get

$$\mathbf{Z}_G \approx \begin{pmatrix} \mathbf{Z}_R + Z_{EE} \begin{pmatrix} 1 \\ \vdots \\ 1 \end{pmatrix} (1 \cdots 1) & Z_{EE} \begin{pmatrix} 1 \\ \vdots \\ 1 \end{pmatrix} \\ Z_{EE} (1 \cdots 1) & Z_{EE} \end{pmatrix} \quad (18)$$

and

$$\mathbf{Y}_G \approx \begin{pmatrix} \mathbf{Y}_R & -\mathbf{Y}_R \begin{pmatrix} 1 \\ \vdots \\ 1 \end{pmatrix} \\ -(1 \cdots 1) \mathbf{Y}_R & Y_{EE} + (1 \cdots 1) \mathbf{Y}_R \begin{pmatrix} 1 \\ \vdots \\ 1 \end{pmatrix} \end{pmatrix} \quad (19)$$

V. Example

We measured \mathbf{Z}_G and \mathbf{Y}_G of an interconnection-ground structure shown in Fig. 4, for $s \approx 1.2 w$ and $h \approx H \approx 0.64 w$. \mathbf{Y}_G is approximately given by $\mathbf{Y}_G = j\omega \mathbf{C}_G$ with

$$\mathbf{C}_G \approx \begin{pmatrix} 116.0 & -3.8 & -0.4 & -0.2 & -95.5 \\ -3.8 & 118.3 & -3.7 & -0.4 & -107.5 \\ -0.4 & -3.7 & 118.3 & -3.8 & -107.9 \\ -0.2 & -0.4 & -3.8 & 115.3 & -96.0 \\ -95.5 & -107.5 & -107.9 & -96.0 & 913.7 \end{pmatrix} \text{ pF/m} \quad (20)$$

Using (13), (15) and (17), we obtain $\mathbf{Y}_R = j\omega \mathbf{C}_R$ with

$$\mathbf{C}_R \approx \begin{pmatrix} 116.0 & -3.8 & -0.4 & -0.2 \\ -3.8 & 118.3 & -3.7 & -0.4 \\ -0.4 & -3.7 & 118.3 & -3.8 \\ -0.2 & -0.4 & -3.8 & 115.3 \end{pmatrix} \text{ pF/m} \quad (21)$$

$$\mathbf{Y}_E = j\omega \mathbf{C}_E \text{ with } \mathbf{C}_E \approx \begin{pmatrix} 16.1 \\ 3.0 \\ 2.6 \\ 14.9 \end{pmatrix} \text{ pF/m} \quad (22)$$

and $\mathbf{Y}_{EE} = j\omega \mathbf{C}_{EE}$ with $\mathbf{C}_{EE} \approx 1284 \text{ pF/m}$. The return conductor is clearly not wide enough to fully shield the TCs from the reference conductor, so that \mathbf{C}_E is not $\mathbf{0}$ pF/m and shows a larger electric external crosstalk coupling for the TCs 1 and 4. At 50 MHz, \mathbf{Z}_G is approximately given by $\mathbf{Z}_G = j\omega \mathbf{L}_G$ with

$$\mathbf{L}_G \approx \begin{pmatrix} 417 & 96 & 73 & 60 & 72 \\ 96 & 424 & 104 & 73 & 84 \\ 73 & 104 & 424 & 97 & 83 \\ 60 & 73 & 97 & 417 & 73 \\ 72 & 84 & 83 & 73 & 101 \end{pmatrix} \text{ nH/m} \quad (23)$$

Using (9), (10) and (11), we obtain $\mathbf{Z}_R = j\omega \mathbf{L}_R$ with

$$\mathbf{L}_R \approx \begin{pmatrix} 375 & 42 & 19 & 17 \\ 42 & 357 & 39 & 18 \\ 19 & 39 & 360 & 43 \\ 17 & 18 & 43 & 374 \end{pmatrix} \text{ nH/m} \quad (24)$$

$$\mathbf{Z}_E = j\omega \mathbf{L}_E \text{ with } \mathbf{L}_E \approx \begin{pmatrix} 30 \\ 17 \\ 18 \\ 29 \end{pmatrix} \text{ nH/m} \quad (25)$$

and $\mathbf{Z}_{EE} = j\omega \mathbf{L}_{EE}$ with $\mathbf{L}_{EE} \approx 101 \text{ nH/m}$. \mathbf{L}_E is not $\mathbf{0}$ nH/m and its entries indicate a significant magnetic external crosstalk coupling for all TCs, at the frequency used for the measurements.

\mathbf{Y}_R and \mathbf{Z}_R may be used to compute voltages and currents in a PDL implementing the ZXnoise method. For instance, if \mathbf{C}_R and \mathbf{L}_R are assumed frequency-independent, we may directly compute the signals and the internal crosstalk voltages shown in Fig. 5, for optimized source and load resistance matrices. The far-end crosstalk voltage shown in Fig. 5 is too high for binary signaling.

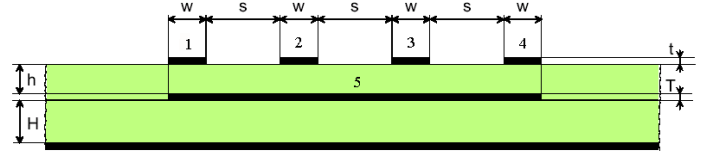


Fig. 4. Cross-section of an interconnection-ground structure built in a printed circuit board, where 1 to 4 are the TCs and 5 is the return conductor.

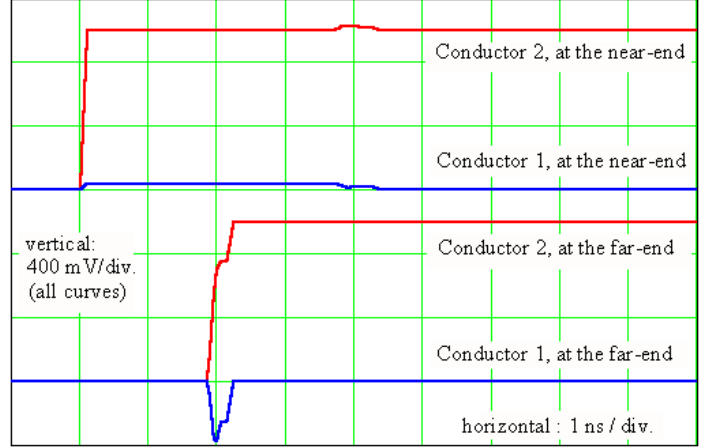


Fig 5. Voltages in a PDL using a 0.3 meter long interconnection, when conductor 2 is excited by a 1V step having a 100 ps rise time.

VI. Conclusion

The matrices \mathbf{Z}_R and \mathbf{Y}_R of the $(n+1)$ -conductor MTL model are adequate for designing PDLs according to the ZXnoise method, because they relate to the natural voltages referenced to the return conductor and the natural currents on the TCs, which are used by the signals propagating on the PDL. However, this model alone does not account for the imperfect shielding action of the return conductor, which leads to external crosstalk. We have shown that the vectors \mathbf{Z}_E and \mathbf{Y}_E characterize this shielding action in the framework of the $(n+1)$ -conductor MTL model and that \mathbf{Z}_E and \mathbf{Y}_E may be derived from a measurement of the matrices \mathbf{Z}_G and \mathbf{Y}_G .

References

- [1] F. Broyd  and E. Clavelier, "A new pseudo-differential transmission scheme for on-chip and on-board interconnections", *Proc. of the CEM 08 Int. Symp. on Electromagnetic Compatibility* (14 me colloque international sur la compatibilit   lectromagn tique - CEM 08), Paris, May 2008, session C7. Available: <http://www.eurexcem.com/biblio.htm>.
- [2] F. Broyd  and E. Clavelier, "Pseudo-differential links using a wide return conductor and a floating termination circuit", *Proc. of the 2008 IEEE International Midwest Symposium on Circuits and Systems (MWSCAS)*, August 10-13, 2008, pp. 586-589.
- [3] F. Broyd  and E. Clavelier, "Comparison of Coupling Mechanisms on Multiconductor Cables", *IEEE Trans. Electromagn. Compat.*, Vol. 35, No. 4, November 1993, pp. 409-416.
- [4] F. Broyd  and E. Clavelier, "Definition, Relevance and Measurements of the Parallel and Axial Transfer Impedances", *Proc. of the 1995 IEEE Int. Symp. on EMC*, Atlanta, August 1995, pp. 490-495.
- [5] F. Broyd  and E. Clavelier, "Characterization of a Cylindrical Screen for External Excitations and Application to Shielded Cables", *IEEE Trans. Electromagn. Compat.*, Vol. 44, No. 4, November 2002, pp. 580-588.